High-Performance Transmission Holographic Gratings via Different Polymerization Rates of Dipentaerythritol Acrylates and Siloxane-Containing Epoxides

Yeong Hee Cho,[†] Chang Won Shin,[‡] Nam Kim,[§] Byung Kyu Kim,[||] and Yusuke Kawakami*,[†]

School of Materials Science, Japan Advanced Institute of Science and Technology (JAIST), 1-1 Asahidai, Nomi, Ishikawa 923-1292, Japan, Prism Technology, Inc., 804 Hakyeonsan Research Center, Chungbuk National University, Cheongju, Chungbuk 361-763, Korea, School of Electrical and Computer Engineering, Chungbuk National University, Cheongju, Chungbuk, 361-763, Korea, and Department of Polymer Science and Engineering, Pusan National University, Pusan, 609-735, Korea

Received May 18, 2005. Revised Manuscript Received October 5, 2005

Well-defined transmission holographic gratings with high diffraction efficiency were fabricated by irradiating a mixture of photopolymerizable materials with different reaction rates consisting of penta-/hexafunctional acrylates and siloxane-containing glycidyl ether (88%) or cyclohexene oxide (85%) as radically and cationically polymerizable monomers, respectively, with Nd:YAG laser ($\lambda = 532$ nm). The ratio between the acrylate and epoxide was important to obtain gratings with high diffraction efficiency. They had smooth surface morphologies of well-regulated spacing (0.9 μm). Performance of holographic gratings was optimized by varying the chemical structures of epoxide under various experimental conditions. Introduction of siloxane component into epoxide induced easy diffusion and distinct separation of the epoxide from the polymerized matrix formed by the acrylate, by their low viscosity and incompatible property during the fabrication of the gratings. These gratings were actually used to store a real image.

Introduction

Optical holography[1−4] recording promises storage density and data-transfer rate which far exceed those of traditional magnetic and optical recordings. There are several types in fabrication of holograms, such as dry film type,[5,6] solution type,[7,8] and liquid crystal (LC) composite type.[9−13] Sutherland[14−17] created the switchable holograms by combining liquid crystals with multifunctional acrylates and explored the electrooptical effects by taking advantage of their large dielectric anisotropy and optical birefringence. High diffraction efficiency approaching 100% was obtained, and the Bragg gratings showed a very narrow angular selectivity (<1°).

Meanwhile, photopolymers are very useful and attractive materials for many applications, such as information storage media,[18−20] as photonic devices,[21−22] and even as photocurable coating materials.[23,24] Kawabata[25] developed a novel photopolymer system consisting of a radically polymerizable monomer (RPM) and a cationically polymerizable monomer (CPM) to write reflection holograms. During the radical polymerization of the RPM by holographic exposure, the CPM remains intact. The remaining liquid CPM enhances the diffusion of the RPM by dilution effect and generated a large modulation of refractive index in the photopolymerized

* To whom correspondence should be addressed. Telephone: + 81-761-51-1630. Fax: +81-761-51-1635. E-mail: kawakami@jaist.ac.jp.
[†] JAIST.
[‡] Prism Technology, Inc., Chungbuk National University.
[§] School of Electrical and Computer Engineering, Chungbuk National University.
[||] Pusan National University.

(1) Heanue, J. F.; Bashaw, M. C.; Hesselink, L. *Science* **1994**, *265*, 749.
(2) Psaltis, D. *Science* **2002**, *298*, 1359.
(3) Shen, X. A.; Nguyen, A.; Perry, J. W.; Huestis, D. L.; Kachru, R. *Science* **1997**, *278*, 96.
(4) Coufal, H. *Nature* **1998**, *393*, 628.
(5) Martin, S.; Feely, C. A.; Toal, V. *Appl. Opt.* **1997**, *36*, 5757.
(6) Calixto, S. *Appl. Opt.* **1987**, *26*, 3904.
(7) Fimia, A.; Lopez, N.; Mateos, F.; Sastre, R.; Pineda, J.; Amat-Guerri, F. *Appl. Opt.* **1993**, *20*, 3706.
(8) Mallavia, R.; Amat-Guerri, F.; Shastre, R. *Macromolecules* **1994**, *27*, 2643.
(9) Park, M. S.; Kim, B. K.; Kim, J. C. *Polymer* **2003**, *44*, 1595.
(10) Sarkar, M. D.; Gill, N. L.; Whitehead, J. B.; Crawford, G. P. *Macromolecules* **2003**, *36*, 630.
(11) Zhai, L.; Nolte, A. J.; Cohen, R. E.; Rubner, M. F. *Macromolecules* **2004**, *37*, 6113.
(12) Kyu, T.; Nwabunma, D. *Macromolecules* **2001**, *34*, 9168.
(13) Zhang, J.; Carlen, C. R.; Palmer, S.; Sponsler, M. B. *J. Am. Chem. Soc.* **1994**, *116*, 7055.
(14) Bunning, T. J.; Natarajan, L. V.; Tondiglia, V. P.; Sutherland, R. L. *Annu. Rev. Mater. Sci.* **2000**, *30*, 83.
(15) Natarajan, L. V.; Shepherd, C. K.; Brandelik, D. M.; Sutherland, R. L.; Chandra, S.; Tondiglia, V. P.; Tomlin, D.; Bunning, T. J. *Chem. Mater.* **2003**, *15*, 2477.
(16) Pogue, R. T.; Sutherland, R. L.; Schmitt, M. G.; Natarajan, L. V.; Siwecki, S. A.; Tondiglia, V. P.; Bunning, T. J. *Appl. Spectrosc.* **2000**, *54* (1), 12A.
(17) Sutherland, R. L.; Natarajan, L. V.; Tondiglia, V. P.; Bunning, T. J. *Chem. Mater.* **1993**, *5*, 1533.
(18) Trentler, T. J.; Boyd, J. E.; Colvin, V. L. *Chem. Mater.* **2000**, *12*, 1431.
(19) Bunning, T. J.; Kirkpatrick, S. M.; Natarajan, L. V.; Tondiglia, V. P.; Tomlin, D. W. *Chem. Mater.* **2000**, *12*, 2842.
(20) Joo, W. J.; Oh, C. H.; Song, S. H.; Kim, P. S.; Han, Y. K. *J. Phys. Chem. B.* **2001**, *105*, 8322.
(21) Yoneyama, S.; Yamamoto, T.; Tsutsumi, O.; Kanazawa, A.; Shiono, T.; Ikeda, T. *Macromolecules* **2002**, *35*, 8751.
(22) Berkovic, G.; Krongauz, V.; Weiss, V. *Chem. Rev.* **2000**, *100*, 1741.
(23) Tomlinson, W. J.; Chandross, E. A.; Weber, H. P.; Aumiller, G. D. *Appl. Opt.* **1976**, *15*, 534.
(24) Hsieh, M. D.; Zellers, E. T. *Sens. Actuators, B* **2002**, *82*, 287.
(25) Kawabata, M.; Sato, A.; Sumiyoshi, I.; Kubota, T. *Proc. SPIE−Int. Soc. Opt. Eng.* **1993**, *66*, 1914.

10.1021/cm051058l CCC: $30.25
Published on Web 11/17/2005

layer. In the subsequent step, an overall exposure, to a different wavelength from the holographic exposure, polymerized the CPM and the remaining RPM, resulting in a stable hologram with high efficiency.

Multifunctional acrylate systems such as DuPont's HRF[26,27] series and Polaroid's DMP-128[28] have been the most widely used for commercial purposes. Both systems provide high-performance and permanently fixed holograms, although they have some drawbacks such as volume shrinkage and multistep processing. Success in further development of holography for various applications depends on the creation of hologram gratings with high resolution and sharp angle selectivity by well-designing the characteristics of the materials used.

Recently, we have focused on the silicon-containing compounds, especially those with silicon−oxygen bonds, as holographic recording materials by taking advantage of their characteristic chemical and physical properties. Actually, in a previous study, silicon-containing epoxide was found effective to induce efficient separation of LC from polymerizable monomer during the formation of gratings and to realize high diffraction efficiency and low volume shrinkage in holographic polymer dispersed liquid crystal (HPDLC) systems.[29]

The objective of this research is to show the effectiveness of siloxane-containing epoxides as CPM in the photopolymer system in the creation of transmittance holographic gratings with high performance by solution process. Siloxane component in CPM was expected to induce its efficient separation into dark regions from the polymer matrix formed by RPM at the position of light interference. Large modulation of refractive index was anticipated due to their incompatibility and difference in refractive index compared with carbon-based matrix materials. Since different grating performance was often seen depending on the formulation of the recording solution, detailed interpretation on grating performance should be made on the precise control of the nature of the recording solution.

In this research, behaviors of CPM with siloxane of definite chain length and cationically polymerizable glycidyl ether or cyclohexene oxide were discussed on the basis of the evaluation of real-time diffraction efficiency under various experimental conditions in the grating formation.

Experimental Section

Materials. *RPM Materials Consisting of a Multifunctional Acrylate and a Reactive Diluent.* Dipentaerythritol penta-/hexaacrylate (MFA) and 1-vinyl-2-pyrollidinone (NVP) were purchased from

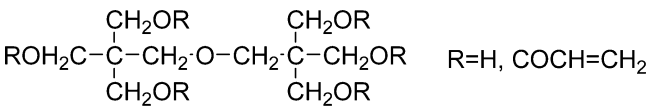

Dipentaerythritol penta-/hexa- acrylate (MFA), n_D^{20}=1.49

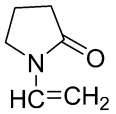

1-Vinyl-2-pyrrolidinone (NVP), n_D^{20}=1.512

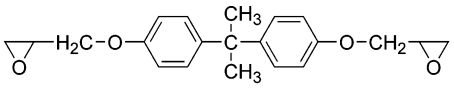

Bisphenol A diglycidylether (**A**)

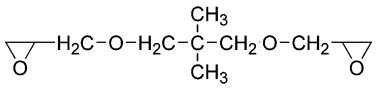

Neopentylglycol diglycidylether (**B**)

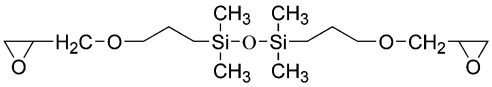

1,3-Bis(3-glycidoxypropyl)-1,1,3,3-tetramethyldisiloxane (**C**)

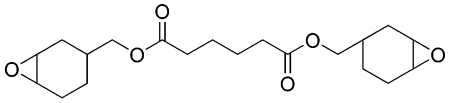

Bis[(1,2-epoxycyclohex-4-yl)methyl] adipate (**D**)

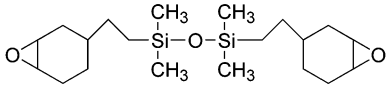

1,3-Bis[2-(1,2-epoxycyclohex-4-yl)ethyl]-1,1,3,3-tetramethyldisiloxane (**E**)

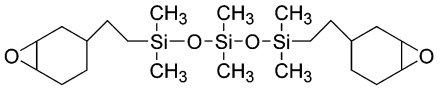

1,5-Bis[2-(1,2-epoxycyclohex-4-yl)ethyl]-1,1,3,3,5,5-hexamethyltrisiloxane (**F**)

Figure 1. Chemical structures of ring-opening polymerizable compounds as CPM.

Aldrich Chemical Co. and used as the multifunctional acrylate to give fast reaction rate and the reactive diluent, respectively. n_D^{20} represents the refractive index as reported in the Aldrich catalog.

CPM Materials. Structures of CPM used in this study are shown in Figure 1. Bisphenol A diglycidyl ether (**A**), neopentyl glycol diglycidyl ether (**B**), and bis[(1,2-epoxycyclohex-4-yl)methyl] adipate (**D**) were purchased from Aldrich. 1,3-Bis(3-glycidoxypropyl)-1,1,3,3-tetramethyldisiloxane (**C**) was purchased from Shin-Etsu Co. and used without further purification.

1,3-Bis[2-(1,2-epoxycyclohex-4-yl)ethyl]-1,1,3,3-tetramethyldisiloxane (**E**) was synthesized by the direct hydrosilylation of 4-vinyl-1-cyclohexene-1,2-epoxide (Aldrich) with 1,1,3,3-tetramethyldisiloxane (Silar Laboratories) in toluene at 60−70 °C for 24 h in the presence of chlorotris(triphenylphosphine)rhodium(I) [$RhCl(PPh_3)_3$] (KANTO Chemical Co. Inc.).[30] Catalyst was removed by passing the reaction mixture through a short silica gel column, and the product was obtained as a colorless oil with low viscosity.

Compound E. ^{1}H NMR ($CDCl_3$) δ (ppm): 0.01 (s, 12H, CH_3-Si), 0.46 (m, 4H, CH_2Si), 0.89−2.19 (m, 18H, other CH_2 and CH), 3.10 (m, 4H, O−CH in epoxy ring).

1,5-Bis[2-(1,2-epoxycyclohex-4-yl)ethyl]-1,1,3,3,5,5-hexamethyltrisiloxane (**F**) was synthesized by hydrosilylation of 4-vinyl-1-cyclohexene-1,2-epoxide with 1,1,3,3,5,5-hexamethyltrisiloxane (Silar) similarly to the synthesis of **E**.

(26) Weber, A. M.; Smothers, W. K.; Trout, T. J.; Mickish, D. J. *Proc. SPIE−Int. Soc. Opt. Eng.* **1990**, *1212*, 30.
(27) Gambogi, W. J.; Weber, A. M.; Trout, T. J. *Proc. of SPIE−Hologr. Imaging Mater.* **1993**, *2043*, 2.
(28) Ingwall, R. T.; Fielding, H. L. *Opt. Eng.* **1985**, *24*, 808.
(29) Cho, Y. H.; He, M.; Kim, B. K.; Kawakami, Y. *Sci. Technol. Adv. Mater.* **2004**, *5*, 319.
(30) Crivello, J. V.; Bi, D. *J. Polym. Sci., Part A: Polym. Chem.* **1993**, *31*, 2563.

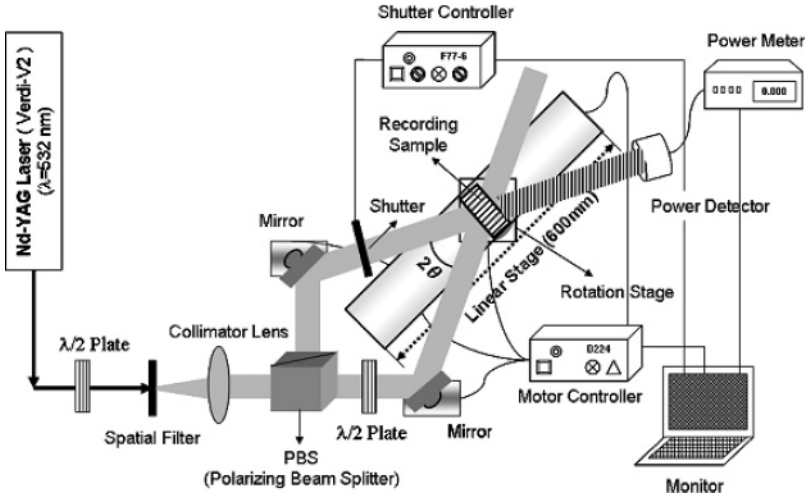

Figure 2. Experimental setup for the holographic recording and real-time reading.

Compound F. ^{1}H NMR ($CDCl_3$) δ (ppm): 0.02 (s, 12H, CH_3-Si), 0.04 (s, 6H, CH_3Si), 0.49 (m, 4H, CH_2Si), 2.0−0.78 (m, 18H, other CH_2 and CH), 3.10 (m, 4H, O−CH in epoxy ring).

Composition of Photosensitive System and Recording Solution. Photoinitiator (PI) and photosensitizer (PS) having sensitivity to visible wavelength of Nd:YAG laser (λ = 532 nm) is required to generate radical or cationic species. Diphenyliodonium hexafluorophosphate (AVOCADO Research Chemicals Ltd.) and 3,3′-carbonylbis(7-diethylaminocoumarin) (Kodak) were selected as a PI and PS, respectively. Good point about this photosensitive system is the insensitivity of cationic polymerization against oxygen. The concentrations of the PI and PS to the recording solution were 0.3−3 and 0.1−0.3 wt %, respectively.

Photosensitizer (PS)

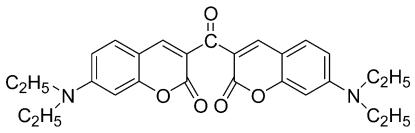

3,3'-Carbonylbis(7-diethylaminocoumarin)

Photoinitiator (PI)

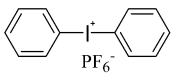

Diphenyliodonium hexafluorophosphate

The recording solution of the photopolymerizable compound was composed of a CPM, a fast-curing MFA, and reactive diluent NVP in the ratio of 20−60, 30−70, and 10 wt %, respectively. The actual concentrations of the reagents in the solution were given in the performance of holographic gratings in Results and Discussion. The recording solution was injected into a glass cell with a gap of 20 μm controlled by bead spacer.

Optical Setup for Transmission Holographic Gratings. Nd:YAG solid-state continuous wave laser with 532 nm wavelength (Coherent lnc., Verdi-V2) was used as the irradiation source as shown in Figure 2. The beam was expanded and filtered by spatial filters and collimated by collimator lens. S polarized beams were generated and split by controlling the two λ/2 plates and polarizing beam splitter (PBS). Thus separated two S polarized beams with equal intensities were reflected by two mirrors and irradiated to recording solution at a predetermined external beam angle (2θ) which were controlled by rotating the motor-driven two mirrors and moving the rotation stage along the linear stage. In this research, the external incident beam angle was set to 16° (θ) against the line perpendicular to the plane of the recording cell. Real-time diffraction efficiency was measured by monitoring the intensity of the diffracted beam when the shutter was closed at a constant time interval during the hologram recording. After the hologram was recorded, diffraction efficiency was measured by rotating the hologram precisely by constant angle by using a motor-driven controller, with the shutter closed to cutoff the reference light, to determine the angular selectivity.

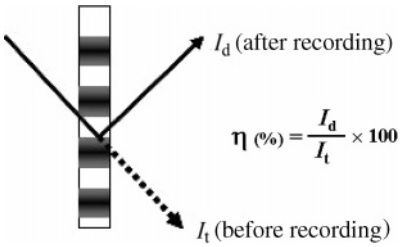

Figure 3. Definition of diffraction efficiency.

Holographic gratings were fabricated under various experimental conditions, by changing laser intensity and irradiation time, and the optimum condition was established to obtain the high diffraction efficiency, high resolution, and excellent long-term stability after recording.

Diffraction Efficiency. The diffraction efficiency is defined as the ratio of diffraction intensity after recording (I_d) to transmitted beam intensity before recording (I_t), as illustrated in Figure 3.

Morphology of Holographic Gratings. The surface morphology of transmission holographic gratings was examined with atomic force microscopy (AFM, JEOL, JSPM-4210). The samples for measurement were prepared by freeze-fracturing in liquid nitrogen, and the AFM was used in tapping mode for image acquisition. A silicon nitride cantilever (Olympus) with a spring constant of 42 N/m and resonant frequency of 300 kHz was used. The morphologies of the samples were examined with a scanning electron microscope (SEM, HITACHI, S-4100). The samples for SEM were prepared by freeze-fracturing in liquid nitrogen, and coating the exposed surface with a very thin layer of Pt−Pd to mininize artifacts associated with sample charging (HITACHI, E-1030 ion sputter).

Results and Discussion

Mechanism of Photoinitiation System. The proposed mechanism of photoinitiation is shown in Scheme 1.[31−33]

(31) Gomurashvili, Z.; Crivello, J. V. *J. Polym. Sci., Part A: Polym. Chem.* **2001**, *39*, 1187.

Scheme 1. Proposed Mechanism of Photosensitizer−photoinitiator System

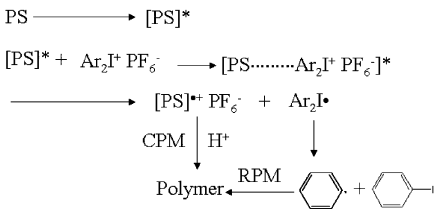

When PS absorbs the laser light and is excited, an excited-state complex (exciplex) is formed as an intermediate between the onium salt and the excited PS. Electron transfer in the exciplex decomposes the exciplex and gives an unstable diaryliodine free radical, which rapidly decomposes to generate aryl radical to induce the radical polymerization of RPM. The photosensitizer cation-radical, or proton generated therefrom, induces the cationic polymerization of CPM.

In the maxima region of the interference fringe, MFA with faster polymerization rate polymerizes first. The polymer formed from MFA is thermodynamically incompatible with CPM and forces CPM out from polymerizing regions to low light intensity regions of the interference fringe. In low light intensity regions, after long-term illumination, the CPM turns to polymer of a solid phase, and refractive index modulation is generated due to their difference in polymerization rate.

Performance of Holographic Gratings. For simple nonslanted transmission gratings, maximum diffraction efficiency is given from Kogelnik's coupled wave theory:[34]

$$\eta = \sin^2[\pi \Delta n T/\lambda \cos \theta]$$

where η is the maximum diffraction efficiency, Δn is the modulation of refractive index of the recording medium after recording, T is the thickness of the hologram, λ is the recording wavelength, and θ is the half-angle of internal incident beams. In this research, T and λ were fixed as 20 μm and 532 nm, respectively. Since the external incident beam angle (θ) was fixed as 16°, the actual internal incident beam angles were about 10° for all samples by calculated Snell's law. Under these conditions, diffraction efficiency was mainly controlled by Δn which could be varied by chemical structure of recording materials. That is to say, when the contrast of refractive index of CPM and RPM materials is large, Δn values also become large if the diffusion of RPM and CPM toward high and low intensity fringes is perfect and the difference of refractive index between monomer and polymer is to be assumed parallel. Large Δn results in large η values.

Refractive index, viscosity, contrast of refractive index, Δn, and maximum diffraction efficiency of the formed gratings for all the CPM are summarized in Table 1.

In evaluating the diffraction efficiency, the ratio of recording solution consisting of MFA, NVP, and CPM was set as 30, 10, and 60 wt %, respectively. The content of PI and PS to the recording solution was 1 and 0.1 wt %, respectively.

Table 1. Refractive Index and Viscosity of CPM, and Maximum Diffraction Efficiency and Generated Δn of the Formed Gratings[a]

structure	n_D^{20} [b]	viscosity (cSt, 25 °C)	contrast of refractive index to RPM (n_{av} [c] = 1.495)	Δn [d]	diffraction efficiency (%)
A	1.586	3450[e]	0.091	0.005 17	33.9
B	1.457	31	0.038	0.007 51	61.7
C	1.452	9	0.042	0.009 22	80.4
D	1.493	664	0.002	0.004 83	30.1
E	1.481	40	0.014	0.006 93	54.8
F	1.474	42−45	0.021	0.007 54	62.0

[a] MFA:NVP:CPM (**A**−**F**) = 30:10:60 (wt %). [b] Refractive index, n_D^{20}, was measured by refractometer (DRM 3000, Otsuka Electronics Co., Ltd.). [c] n_{av}: average of refractive index of RPM. [d] Modulation refractive index, Δn, was calculated by Kogelnik's equation, and the actual internal incident beam angles were calculated by Snell's law. [e] Dow Plastics.

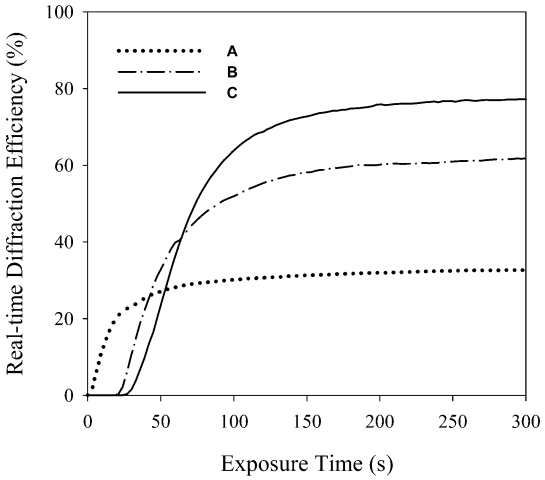

Figure 4. Real-time diffraction efficiency of the gratings formed with bis-(glycidyl ethers)s as CPM at a constant concentration of 1 wt % PI and 0.1 wt % PS, and at 40 mW/cm^2 intensity with MFA:NVP:CPM (**A**−**C**) = 30:10:60 (wt %).

It is possible to select CPM with higher refractive index or lower refractive index than the average of refractive index of RPM. By the evaluation of real-time diffraction efficiency (Figure 4) the effects of the chemical structures of CPM on formation of holographic gratings can be understood.

Diffraction efficiency for diglycidyl ether derivatives increased in the order of **A** < **B** < **C**, although contrast of refractive index increased in the order of **B** < **C** < **A**. **A** showed the smallest Δn and **C** the largest.

It may be considered that after the initial diffusion of **A** caused by the polymerization of MFA, further diffusion of **A** seemed to be interfered with due to its high viscosity, as shown in Table 1. Diffusion of MFA to high-intensity fringes was also suppressed. Since the viscosity of recording solution was too high, there was not enough time for MFA and **A** to diffuse out to high- and low-intensity fringes, respectively, and they were trapped in a highly cross-linked region and will not contribute to high Δn.

On the contrary, **B** induced higher diffraction efficiency than **A**, although the contrast of refractive index was lower than **A**. This can be considered that **B,** having a lower molecular weight and a more flexible structure than **A** with bulky benzene ring, gave less viscous recording solution and made the diffusion of MFA and **B** easy toward high-intensity and low-intensity fringes, respectively.

(32) Crivello, J. V.; Jiang, F. *Chem. Mater*. **2002**, *14*, 4858.
(33) Gomurashvili, Z.; Crivello, J. V. *Macromolecules* **2002**, *35*, 2962.
(34) Kogelnik, H. *Bell Syst. Technol. J*. **1969**, *48*, 2909.

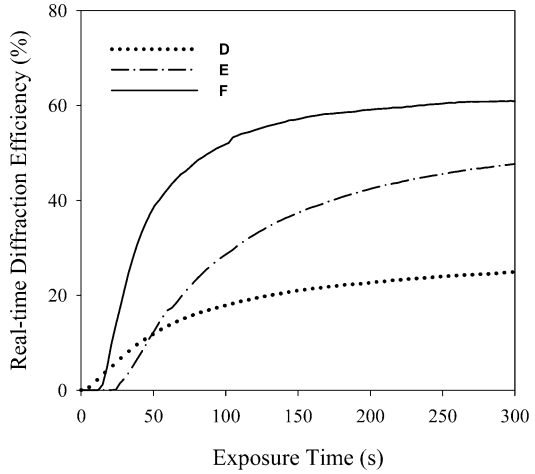

Figure 5. Real-time diffraction efficiency of the gratings formed with bis(cyclohexene oxide) derivatives as CPM at constant concentration of 1 wt % PI and 0.1 wt % PS, and at 40 mW/cm^2 intensity with MFA:NVP:CPM (**D**−**F**) = 30:10:60 (wt %).

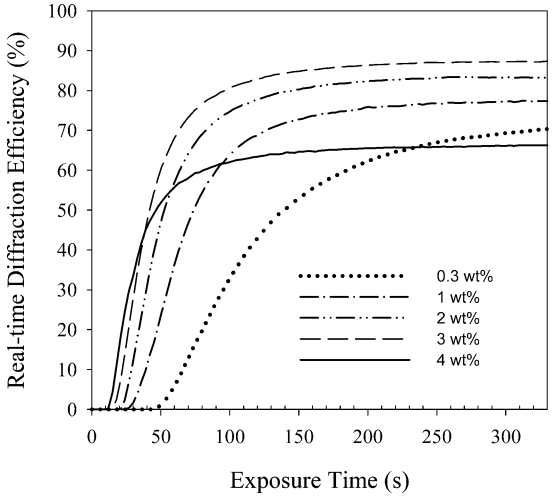

Figure 6. Effects of PI concentration on real-time diffraction efficiency of the gratings formed with **C** at 0.1 wt % PS and at 40 mW/cm^2 intensity with MFA:NVP:CPM (**C**) = 30:10:60 (wt %).

In the case of recording with **C** having siloxane chain, much higher diffraction efficiency was obtained than the case of **B**, irrespective of its longer chain length and higher molecular weight. It may be considered that **C** easily diffused to lower intensity fringes as the polymerization of MFA proceeded due to its flexible and incompatible properties. The flexible chain also helped the further diffusion of remaining MFA and **C** to high- and low-intensity fringes, respectively, which resulted in higher Δn even with somewhat longer exposure time.

As shown in Figure 4, the induction period of grating formation became longer in the order of **A** < **B** < **C**. Generally, in grating formation by radical polymerization, the induction period is observed because polymerization does not begin in the presence of oxygen, which acts as an inhibitor. When the dissolved oxygen in the system is completely consumed, polymerization starts.

In the present system, the induction period for grating formation should also depend on the viscosity of recording solution related to the chemical structure of CPM and the polymerization rate and cross-linking density of RPM. In the present study, RPM was fixed as MFA and NVP at constant concentration; thus, induction periods were varied by the physical property and chemical structures of the CPM. It would be reasonable to consider that the recording solution with **A** had the shortest induction period because of its highest viscosity and by trapping **A** in the matrix, and that with **C** the longest because of the easiest diffusion of **C** due to its lowest viscosity given by siloxane chain.

In the present photopolymerizable system, Δn, which plays an important role in determining the diffraction efficiency, depends not only on the static contrast of refractive index between MFA and CPM but also on the dynamic separation process between RPM and CPM. For high diffraction efficiency and short induction period, the importance of the balance between the separation of RPM and CPM through diffusion and the polymerization rate should be stressed.

Figure 5 shows the real-time diffraction efficiency of the gratings formed with bis(cyclohexene oxide) derivatives as CPM.

Compound **D** had the lowest diffraction efficiency due to its lowest contrast of refractive index and highest viscosity (Table 1). Compound **E** showed about 55% diffraction efficiency. The highest diffraction efficiency over 62% was obtained for **F**. Although the order of diffraction efficiency was in accordance with the order of the contrast of refractive index, it seemed that, as mentioned above, siloxane chain in **E** and **F** made the solution less viscous, and incompatibility with MFA, which helped the easy diffusion and good separation between RPM (MFA) and CPM, and high Δn was attained. Especially, **F** showed higher diffraction efficiency than **E** probably due to flexibility and incompatibility brought about by its longer siloxane chain. However, compared with **C**, **F** did not give higher diffraction efficiency, even with longer siloxane chain. It may be understood that **F** has more bulky cyclohexene oxide functional group, and its diffusion is not easier compared with **C.** It may have a faster polymerization rate than **C**.[35] Accordingly, only a part of **F** could be polymerized in high-intensity fringes; therefore, high Δn could not be obtained.

The induction period of grating formation increased in the order of **D** < **F** < **E**, which was consistent with the above discussion**.** Further study for **F** should be done in order to optimize the diffraction efficiency by varying the ratio of RPM/CPM and the concentration of reactive diluent. However, **F** could not be mixed with other reagents in an arbitrary ratio. According to the limitation of the solubility of PI in the recording solution, especially, in the case of **F**, 1 wt % PI was used in the above formulation (Figure 4 and Figure 5).

Effects of the Concentration of Photoinitiator on Real-Time Diffraction Efficiency. The PI concentration was varied from 0.3 to 4 wt % with a constant concentration of 0.1 wt % PS in formulation MFA:NVP:CPM (**C**) = 30:10:60 (wt %). As shown in Figure 6, in increasing the PI concentration from 0.3 to 4 wt %, the induction period of grating formation was markedly shortened, and the diffraction efficiency was the highest with 3 wt % PI and then a little

(35) Crivello, J. V.; Lee, J. L. *J. Polym. Sci., Part A: Polym. Chem.* **1990**, *28,* 479.

decreased with 4 wt % PI. It may be understood that if the PI concentration is low, the number of radicals produced is too low compared with the number of reactive sites available. Furthermore, a part of the radicals might be consumed by inhibiting inpurity. As the concentration increases, the number of radicals produced per unit time and per unit volume will increase and an optimum curing rate is obtained. Above a certain point (in this case 3 wt %), there exist excess initiating radicals compared to the reactive sites available and no further increase in initiator and diffraction efficiencies will be observed. A slight decrease might be attributed to the termination of propagating species by initiating radicals existing in excess. The reaction can even be retarded if termination steps become dominant due to a high concentration of free radicals. From these considerations it becomes clear that, ideally, the optimum number of radicals should be produced uniformly throughout the solution in cell to be cured during the recording process. In the present recording formulation, the optimum concentration of PI is 3 wt %.[36]

Effects of the Intensities of Incident Beams on Diffraction Efficiency. In radical photopolymerization systems, the polymerization rate (R_p) is proportional to the illumination intensity:[37]

$$R_p = (\Phi I_0[A]x)^{\delta}(k_p/2k_t^{1/2})[M]$$

where Φ is the overall initiation efficiency of the process, I_0 is the illumination intensity, [A] is the concentration of the species that undergo photoexcitation, x is the thickness of the system being irradiated, and δ is the value determined by reaction environments. The coefficients k_p and k_t are the rate constants of chain propagation and termination, respectively, and [M] is the concentration of monomer.

According to Kogelnik's coupled wave theory, diffraction efficiency should be changed as a sinusoidal mode by modulation of refractive index caused by photopolymerization controlled by the intensity of the light. The intensity of the incident beam was varied so as to optimize the effect of the reaction rate of RPMs on diffraction efficiency of the gratings formed by with **C**, 3 wt % PI and 0.3 wt % PS.

The maximum diffraction efficiency of the final grating was changed roughly as a sinusoidal pattern depending on the intensity of the incident beams even at very low intensities of 0.8 and 1.4 mW/cm^2 and diffraction efficiencies of 62 and 84% were obtained, respectively. In Figure 7, dependence of real-time diffraction efficiency on the intensity of incident beam was shown. Under a very low intensity of 0.8 mW/cm^2, the polymerization rate of MFA itself became very slow to form grating, resulting in the very gentle slope. On the contrary, under the high intensity of 10 mW/cm^2, the polymerization rate of MFA was fast enough to form grating in short exposure time and showed a very rapid slope. By varying the intensity of the incident beam from 0.8 to 10 mW/cm^2, the induction period of grating formation was shortened gradually from about 126 to 18 s.

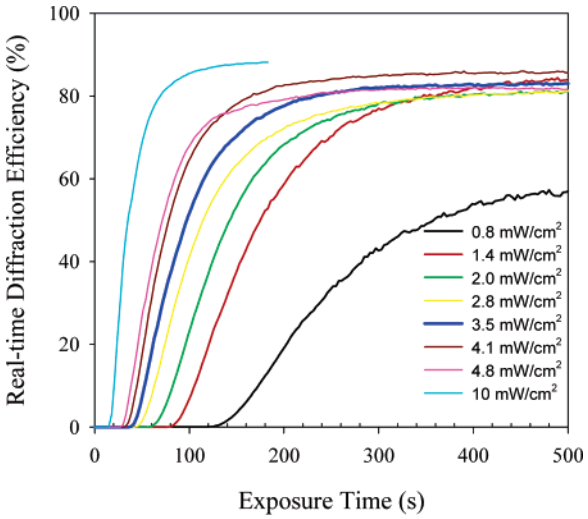

Figure 7. Effects of intensity of irradiation beams on real-time diffraction efficiency of holographic gratings formed with **C** (MFA:NVP:CPM (**C**) = 30:10:60 (wt %)).

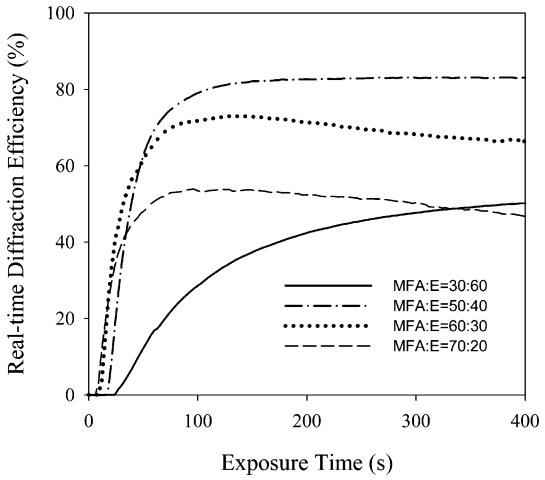

Figure 8. Effects of ratio of MFA and **E** on real-time diffraction efficiency of the gratings at the ratios of MFA:**E** from 30:60 to 70:20 (wt %) and at 40 mW/cm^2 intensity with 1 wt % PI and 0.1 wt % PS.

Effects of the Ratio of MFA and CPM on Real-Time Diffraction Efficiency. Holographic gratings of the present system are mainly formed by photopolymerization of MFA and diffusion and following polymerization of CPM as mentioned above. The ratio of MFA and CPM plays an important role in forming the gratings with high diffraction efficiency, since the polymerization rate and cross-linking density of MFA depend on the concentration of MFA. To improve the diffraction efficiency of the MFA−**E** system, which showed a lower diffraction efficiency (55%) than the MFA−**C** system (85%), the ratio of MFA:**E** was changed, and the result was shown in Figure 8.

The ratio of MFA:**E** was varied from 30::60 to 70:20 (wt %) at constant concentration of 10 wt % NVP. Two different concentrations of 1 wt % PI and 0.1 wt % PS were also used in the recording solution. By increasing the concentration of MFA from 30 to 50 wt %, the final diffraction efficiency increased from 55 to 84% and decreased to about 38% by further increase in the concentration of MFA to 70 wt %. When the concentration of MFA is too high, or the content of **E** is too low, gelation of the recording materials formed in very short time; thus, MFA and **E** were

(36) Crivello, J. V.; Dietliker, K. *Photoinitiators for Free Radical Cationic and Anionic Photopolymerisation*, 2nd ed.; John Wiley and Sons: London U.K., 1998.
(37) Mishra, M. K.; Yagci, Y. *Handbook of Radical Vinyl Polymerization*; Marcel Dekker lnc.: New York, 1998.

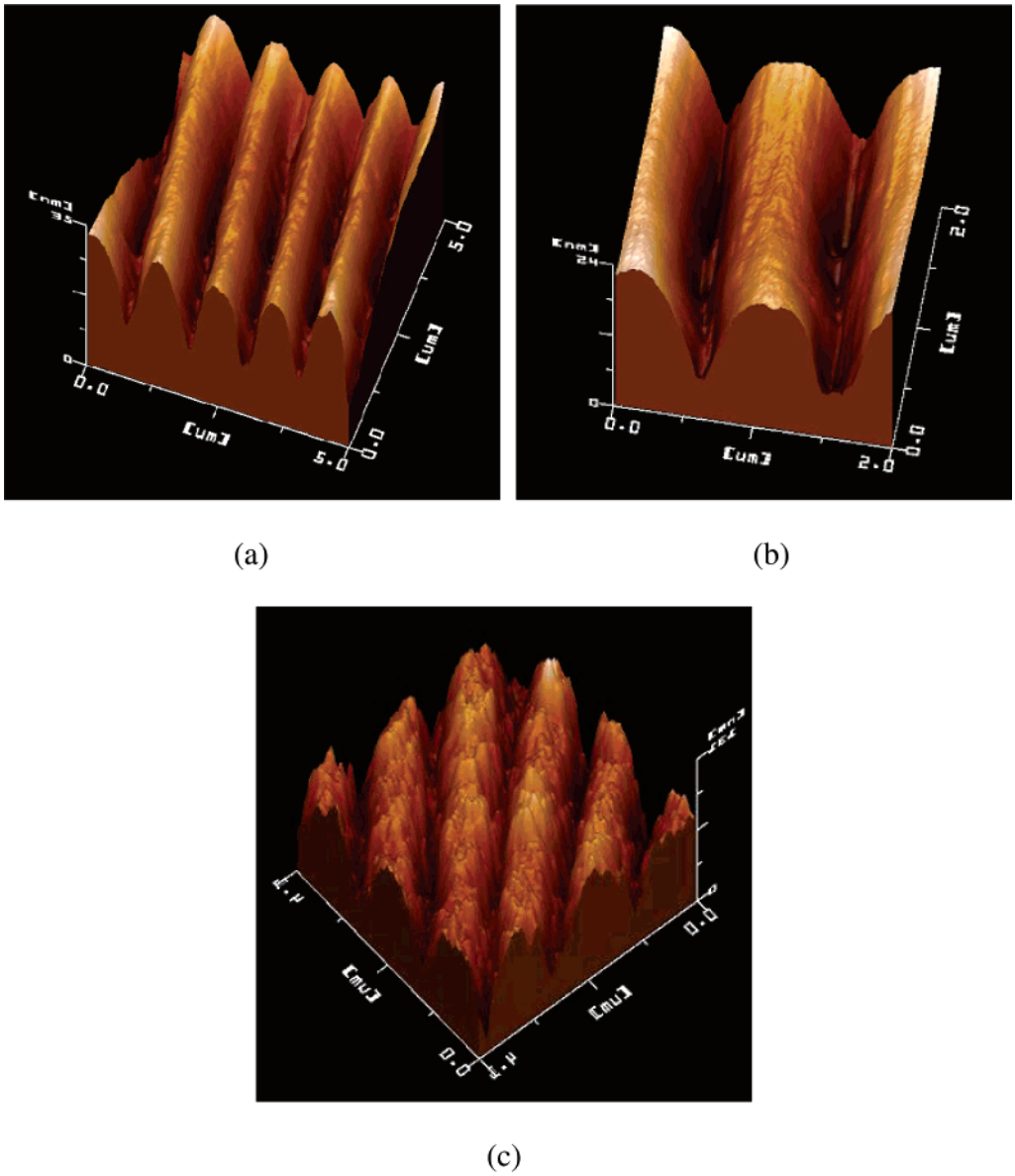

Figure 9. AFM surface topology of transmission holographic gratings formed with siloxane-containing epoxide derivatives as CPM: (a) **C**, (b) magnification of **C**, and (c) **E**.

trapped in a highly cross-linked region and lose their mobility in the course of the polymerization reaction; consequently, large Δn should not be generated and resulted in the decrease of the final diffraction efficiency. The slight decrease in diffraction efficiency during the exposure might be attributed to the initial fast nonequibrium cross-linking followed by the relaxation of the structure.

AFM Surface Topology of Formed Gratings. The surface topologies of the gratings are shown in Figure 9.

The grating of high diffraction efficiency formed with **C** shown in Figure 9a was more clearly formed with over 80% diffraction efficiency than those of **E** in Figure 9c at the same MFA:NVP:CPM ratio. It was considered that **C**, having lower viscosity, easily diffused toward low-intensity fringes and helped good separation between RPM and CPM, resulting in clear gratings. The magnified image of Figure 9a is shown in Figure 9b, which showed about 0.9 μm grating spacing. This value was in good agreement with the calculated spacing (0.96 μm) by Bragg's equation. As shown in Figure 9c, gratings formed with **E** showed a little rough surface. For the formation of holographic gratings of high diffraction efficiency, it is very important to control the difference in polymerization rate between RPM (MFA) and CPM. If the reaction rate of a CPM is too fast, some CPM and MFA are left in the high-intensity fringes, and precise modulation cannot be generated, as discussed previously. It is worthwhile to comment that the smoothness of the grating surface is in the same trend with the order of the diffraction efficiency, although they are not directly related, since refractive index modulation determines the diffraction efficiency.

SEM Morphology of Formed Gratings. Well-defined structure of the transmission holographic gratings fabricated with **C** as CPM was evidenced by SEM observation. As can be seen in Figure 10, clear layered structures were observed not only as a surface view but also as cross-sectional view. We can even see the partly fractured cross-sectional layers slipped out from the inner layered structure in the surface

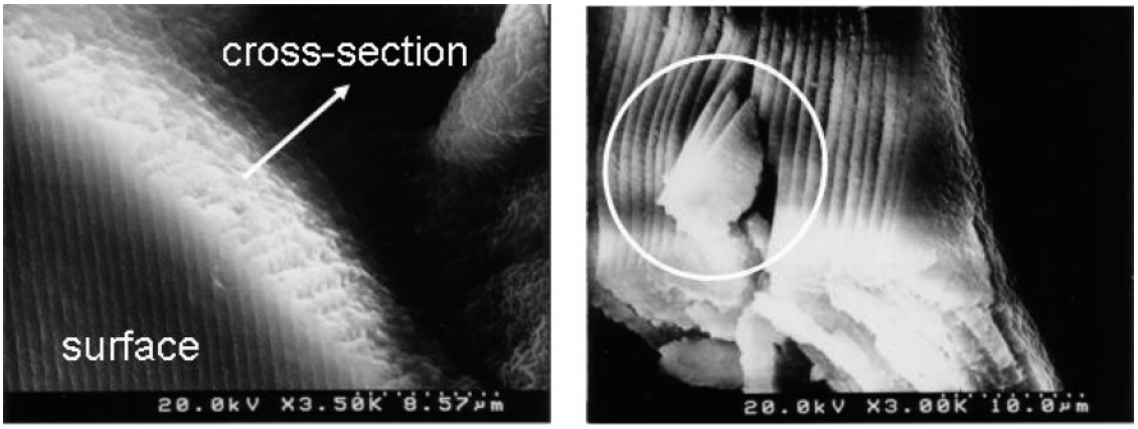

Figure 10. Morphologies of the gratings formed with **C** as siloxane-containing CPM (a) surface and cross-sectional views and (b) slipped out cross-sectional layers from the inner layers.

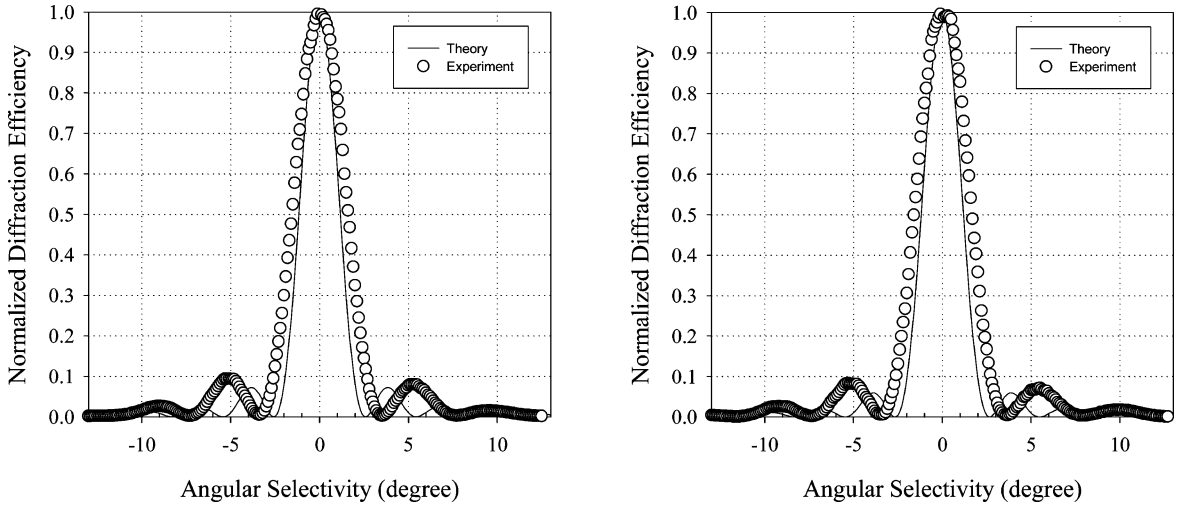

Figure 11. Angular selectivity for holographic gratings formed from (a) **C** and (b) **E**.

view, as shown in Figure 10b. Apparently, in the lowest intensity regions of interference, only slight or no cross-linking occurred by the polymerization of RPM or CPM. Of course, this may be undesirable from the viewpoint of stability, but this figure gives very good evidence for the formation of gratings with layered structure in the present systems.

Angular Selectivity. When the multiplex hologram is to be recorded, it is very important to have sharp angular selectivity. The smaller the value, the more multiplex data or gratings can be recorded.

As typically shown in Figure 11, angular selectivities ($\Delta\theta_{ang}$) were similar for all samples, irrespective of the structures of epoxides (about 3.4°). This value is in good agreement with theoretical value according to the Kogelnik's coupled wave theory, as follows:

$$\Delta\theta_{ang} = \frac{1}{2n \sin\theta}\sqrt{\left[\left(\frac{\lambda}{T}\right)^2 - \left(\frac{\Delta n}{\cos\theta}\right)^2\right]}$$

where n is the average refractive index of recording solution, θ is the internal incident beam angle, T is the thickness of the hologram, λ is the recording wavelength, and Δn is the modulation of refractive index of the recording solution after recording.

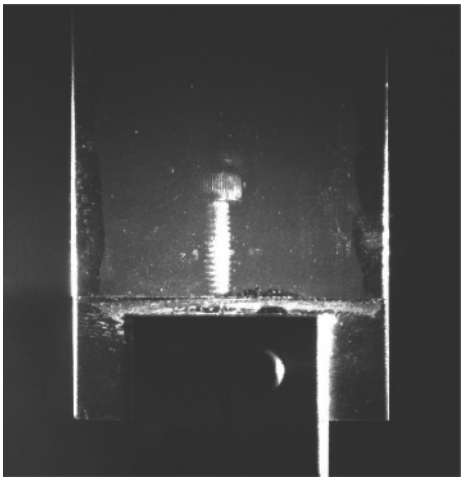

Figure 12. Real image of a screw recorded in photopolymerizable material with **C** as CPM.

Adjustment of the sample thickness and interbeam angle is needed to further reduce the angular selectivity.

Storage of Real Image of Screw. Real images of a screw were successfully stored using photopolymerizable materials with **C** having siloxane chain and captured by CCD camera, which showed a very clear and stable image when only the

reference beam was irradiated into the sample, as shown in Figure 12.

Conclusion

We have demonstrated the formation of holographic gratings via different reaction and diffusion rates using epoxides with various chemical structures as CPM. By controlling the chemical structures, concentration, and the reaction rate, the optimum condition with high diffraction efficiencies was established. Especially, siloxane-containing CPM induced good diffusion and separation during the formation of holographic gratings.

By varying the functional group of CPM, gratings with much higher performance could be obtained as in the case with **C** having a glycidyl ether function. Well-fabricated gratings with very regular and clean morphology and high diffraction efficiency over 88% were obtained. The lower diffraction efficiency with **E** (55%) could be improved (84%) by adjusting the ratio of MFA and **E**. Gratings with angular selectivity of $<3.4°$ were prepared and real image of a screw was stored successfully with these systems.

Acknowledgment. This work was partly supported by a Grant-in-Aid for Scientific Research (16205016) from the Ministry of Education, Science, Sports, Culture and Technology, Japan. This work was also carried out partly in the Nanotechnology Glass Project, as part of the Nanotechnology Materials Program supported by the New Energy and Industrial Technology Development Organization (NEDO).

CM051058L